Neural Networks 24 (2011) 592–601

Contents lists available at ScienceDirect

Neural Networks

journal homepage: www.elsevier.com/locate/neunet

2011 Special Issue

Origins of a repetitive and co-contractive biphasic pattern of muscle activation in Parkinson's disease

Vassilis Cutsuridis

Center for Memory and Brain, Boston University, Boston, MA 02215, USA

ARTICLE INFO

Keywords:
Parkinson's disease
Triphasic pattern of muscle activation
Co-contraction
Dopamine
Globus pallidus
Cortex
Spinal cord

ABSTRACT

In studies of electromyographic (EMG) patterns during movements in Parkinson's disease, often a repetitive and sometimes co-contractive pattern of antagonist muscle activation is observed. It has been suggested that the origin of such patterns of muscle activation is a central one arising from impairments in the basal ganglia structures and/or the cortex, although afferent inputs can also modulate the voluntary activity. A neural network model of Parkinson's disease, bradykinesia and rigidity, is extended to quantitatively study the conditions under which such a repetitive and co-contractive pattern of muscle activation appears. Computer simulations show that an oscillatory disrupted globus pallidus internal segment (GPi) response signal comprising at least two excitation–inhibition sequences as an input to a normally functioning cortico-spinal model of movement generation results in a repetitive, but *not* co-contractive agonist–antagonist pattern of muscle activation. A repetitive *and* co-contractive pattern of muscle activation results when also dopamine is depleted in the cortex. Finally, additional dopamine depletion in the spinal cord sites results in a reduction of the size, duration and rate of change of the repetitive and co-contractive EMG bursts. These results have important consequences in the development of Parkinson's Disease therapies such as dopamine replacement in cortex and spinal cord, which can alleviate some of the impairments of Parkinson's Disease such as slowness of movement (bradykinesia) and rigidity.

1. Introduction

Voluntary movements are goal-directed movements triggered either by internal or external cues. Single-joint rapid (ballistic) movements are one type of goal-directed movements performed "as fast as possible" or "as fast and as accurate as possible" in a single action without the need for corrective adjustments during their course. They are characterized by a symmetric bell-shaped velocity curve, where the acceleration and deceleration times are equal (Britton et al., 1994). Similar velocity profiles have also been observed in multi-joint movements (Camarata et al., 1992).

The electromyographic (EMG) pattern of single-joint rapid voluntary movements in normal subjects is very characteristic. It is characterized by alternating bursts of agonist and antagonist muscles (Hallett, Shahani, & Young, 1975). The first agonist burst provides the impulsive force for the movement, whereas the antagonist activity provides the braking force to halt the limb. Sometimes a second agonist is needed to bring the limb to its final position (Berardelli, Dick, Rothwell, Day, & Marsden, 1986; Brown & Cooke, 1984, 1990a, 1990b; Ghez & Gordon, 1987a, 1987b, 1987c; Gottlieb, Latash, Corcos, Liubinskas, & Agarwal, 1992; Hallett & Marsden, 1979; Pfann, Hoffman, Gottlieb, Strick, & Corcos, 1998; Wierzbicka, Wiegner, & Shahani, 1986). The combination of the agonist–antagonist bursts is known as the *biphasic or triphasic pattern* of muscle activation (Hallett et al., 1975).

The origin of the biphasic/triphasic pattern and whether it is controlled by the nervous system has been long debated (Stein, 1982). Berardelli et al. (1986) suggested that: (1) the basal ganglia output plays a role in the scaling of the first agonist burst size, (2) the cortico-spinal tract has a role in determining spatial and temporal recruitment of motor units, and (3) the proprioceptive feedback is not necessary for the production of the triphasic pattern, but it contributes to the accuracy of both the trajectory and the end-point of ballistic movements. That means that the origin of the triphasic pattern of muscle activation *may* be a central one, but afferent inputs can also modulate the voluntary activity.

In Parkinson's disease (PD) the biphasic/triphasic pattern of muscle activation is disrupted requiring multiple cycles of EMG bursts to bring the limb to its final target (Berardelli et al., 1986, Hallett & Khoshbin, 1980, Vaillancourt et al., 2006, Vaillancourt, Prodoehl, Veragen-Metman, Bakay, & Corcos, 2004). Some studies have shown that the duration of the bursts is normal, and the bursts increase in duration and amplitude with increasing movement distance (Berardelli et al., 1986, Vaillancourt et al., 2006, 2004).

E-mail address: vcut@bu.edu.

0893-6080/$ – see front matter © 2011 Elsevier Ltd. All rights reserved.
doi:10.1016/j.neunet.2011.03.008

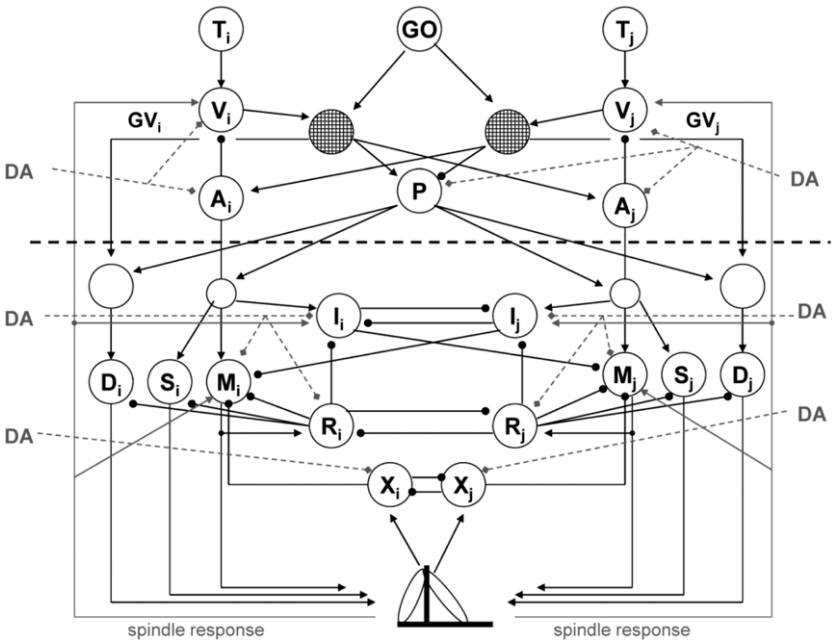

Fig. 1. Neural architecture of the dopamine modulated cortico-spinal model with muscle spindle feedback to cortex. *Top*: Cortical module for trajectory formation. *Bottom*: Opponent processing spinomuscular module. *Arrow black lines*: excitatory projections; *Solid dot black lines*: inhibitory projections; *Diamond-dotted gray lines*: dopamine modulation; *Solid arrow gray lines*: feedback pathways from muscle spindles. *GO*: globus pallidus internal segment (GPi) output signal; *P*: bidirectional co-contractive signal; *T*: target position command; *V*: DV activity; *GV*: DVV activity; *A*: current position command; *M*: alpha motoneuronal activity; *R*: Renshaw cell activity; *X*: spinal type b inhibitory interneuronal activity; *I*: spinal type a inhibitory interneuronal activity; *S*: static γ_{MN} activity; *D*: dynamic γ_{MN} activity; *i*, *j*: antagonist cell pair.

In contrast, (Hallett & Khoshbin, 1980) observed that the EMG patterns in PD subjects differed from those of the healthy subjects in that the bursts of EMG activity did not increase in magnitude for the larger amplitude movements. Many hypotheses have been put forward to explain the slowness in single degree-of-freedom (DF) movement in PD: reduced ability to modulate the magnitude of the agonist EMG burst (Hallett & Khoshbin, 1980), inappropriate scaling of the agonist EMG burst leading to an agonist burst reduced area (Berardelli et al., 1986) and decrease in rate of rise of the agonist burst (Godaux, Koulischer, & Jacquy, 1992).

Similarly, in 1-methyl-4-phenyl-1,2,5,6-tetrahydropyridine (MPTP)-treated animal studies (Benazzouz, Gross, Dupont, & Bioulac, 1992; Doudet, Gross, Arluison, & Bioulac, 1990), where monkeys were trained to perform fast flexion and extension elbow movements, additional successive bursts of lower amplitude and duration were needed for the monkeys to achieve the full amplitude of the required movement. Benazzouz et al. (1992) showed multiple co-activations of antagonist muscles.

Cutsuridis and Perantonis (2006) were the first to offer computationally a plausible hypothesis of why PD EMG agonist burst activity is reduced and why on some occasions multiple agonist–antagonist–agonist bursts are needed to complete the movement. They proposed that disruptions of GPi neuronal activity (Tremblay, Filion, & Bedard, 1989) and dopamine depletion in the cortex and spinal cord disrupt the reciprocal organization of primary motor cortical neurons, reduce their activity, and decrease their rate of change resulting in the downscaling of the size of the first agonist burst and in the decrease of its rate of change. So, in order for the subject to complete the movement and reach the target, additional EMG bursts are required. However, they failed to see a co-contractive pattern of muscle activation (see Figure 10 in Cutsuridis and Perantonis (2006)). In a subsequent modeling study, Cutsuridis (2007) investigated the effects of muscle spindle feedback on key cortical cells and examined the effects of dopamine depletion on spinal activities. Simulation results showed that although reciprocal inhibition is reduced in DA depleted case, this *still* does not lead to a co-contraction of antagonist motoneurons. Cutsuridis (2007) concluded that causes of motoneuronal co-contraction need to be searched more centrally, potentially in the motor cortex and/or the basal ganglia.

In the present work, I will start from the conclusion of the Cutsuridis (2007) study and attempt more systematically to show the conditions under which a repetitive *and* co-contractive biphasic pattern of muscle activation appears. Computer simulations will show that an oscillatory disrupted globus pallidus internal segment (GPi) response signal as an input to a normally functioning cortico-spinal model of movement generation results in a repetitive, but *not* co-contractive agonist–antagonist pattern of muscle activation. A repetitive and co-contractive pattern of muscle activation results when also dopamine is depleted in the cortex. Finally, additional dopamine depletion in the spinal cord sites results in a reduction of the size, duration and rate of change of the repetitive and co-contractive EMG bursts.

2. Methods

2.1. The model and its mathematical formalism

Fig. 1 depicts the components of the dopamine innervated opponent processing cortico-spinal network with spindle feedback to the cortex. Experimental evidence of the connectivity and physiology of the model's elements can be found in Cutsuridis (2007). Experimental evidence of the DA innervation of the neocortex and spinal cord has been detailed in Cutsuridis (2006, 2007, 2010), Cutsuridis and Perantonis (2006).

All of the equations (Eqs. (1)–(4), (6), (8)–(11), (13)–(20), (22) and (23)) presented in this section have been introduced before in Cutsuridis (2007). Eqs. (5), (7), (12) and (21) from Cutsuridis (2007) have been modified in this paper. In this Section 1 list all equations (old and modified) in order to enhance the readability of the paper and help its readers.

The output of the basal ganglia structures, which is represented by the activity of the globus pallidus internal segment (GPi) is

modeled by a GO signal

$$G(t) = G_0(t - \Im_i)^2 u[t - \Im_i]/(\beta + \gamma(t - \Im_i)^2) \quad (1)$$

where G_0 amplifies the GO signal, $\Im_i$ is the onset time of the ith volitional command, β and γ are free parameters, and $u[t]$ is a step function that jumps from 0 to 1 to initiate movement. The difference vector (DV) between the target position vector T and the current position vector A, is described by

$$\frac{dV_i}{dt} = 30(-V_i + T_1 - DA_1 \cdot A_i + DA_1 \cdot a_w \cdot (W_i(t-\tau) - W_j(t-\tau))) \quad (2)$$

$$\frac{dV_j}{dt} = 30(-V_j + T_2 - DA_1 \cdot A_j + DA_1 \cdot a_w \cdot (W_j(t-\tau) - W_i(t-\tau))) \quad (3)$$

where T_1 and T_2 are the target position commands, A is the current limb position command, a_w is the gain of spindle feedback, DA_1 is the modulatory effect of dopamine on area PPV inputs to DV cell activity and indices i and j designate antagonist neuronal populations. Dopamine's values can range from 0 (lesioned) to 1 (normal). The desired velocity vector (DVV), which represents area's 4 reciprocally activated cell activity (Doudet et al., 1990), is defined by

$$u_i = [G \cdot (DA_2 \cdot V_i - DA_3 \cdot V_j) + B_u/DA_4]^+ \quad (4)$$

$$u_j = [G \cdot (DA_2 \cdot V_j - DA_3 \cdot V_i) + B_u/DA_4]^+ \quad (5)$$

where i, j designate opponent neural commands, B_u is the baseline activity of the phasic-MT area 4 cell activity, and DA_2, DA_3, are the modulatory effects of dopamine on DV inputs to DVV cell activity and DA_4 is the effect of dopamine on DVV baseline activity. The co-contractive vector (P), which is represented by area's 4 bidirectional neuronal activity (Doudet et al., 1990) is given by

$$P = [G \cdot (DA_2 \cdot V_i - DA_3 \cdot V_j) + B_P/DA_4]^+. \quad (6)$$

The present position vector (PPV) dynamics is defined by

$$\frac{dA_i}{dt} = (1 - A_i) \cdot (u_i - u_j) - A_i \cdot (u_j - u_i) \quad (7)$$

$$\frac{dA_j}{dt} = (1 - A_j) \cdot (u_j - u_i) - A_j \cdot (u_i - u_j). \quad (8)$$

The quadratic force–length relationship of muscle is approximated by

$$F_i = k([L_i - \Gamma_i + C_i]^+)^2 \quad (9)$$

$$F_j = k([L_j - \Gamma_j + C_j]^+)^2 \quad (10)$$

where k is a scaling parameter, F is muscle force, L is muscle length, Γ_i and Γ_j are the resting muscle lengths, C is muscle contractile state. The contractile state dynamics is defined by

$$\frac{dC_i}{dt} = \beta_i[(B_i - C_i) \cdot [M_i]^+ - \delta \cdot C_i] - [F_i - \Gamma_F]^+ \quad (11)$$

$$\frac{dC_j}{dt} = \beta_j[(B_j - C_j) \cdot [M_j]^+ - \delta \cdot C_j] - [F_j - \Gamma_F]^+ \quad (12)$$

where Γ_F is the force threshold, M is the alpha-motoneuron (α-MN) pool activity, β is the contractile rate, and B is the number of contractile fibers recruited. The muscle lengths for opponent biceps (BIC) and triceps (TRI) muscles are

$$L_i = \sqrt{(20 - \sin(\Theta))^2 + (\cos(\Theta)^2)} \quad (13)$$

and

$$L_j = \sqrt{((20 + \sin(\Theta))^2 + (a\cos(\Theta))^2)} \quad (14)$$

where L_i and L_j are the lengths of the BIC and TRI muscles and Θ is the angle of rotation. The limb dynamics is defined by

$$\frac{d^2\Theta}{dt^2} = \left(F_i - F_j + F_e - \eta\frac{d\Theta}{dt}\right)/I_m \quad (15)$$

where F_e is the external force, η is the viscosity and I_m is the moment of inertia. The contraction rate is defined by

$$\beta_i = 0.05 + 0.01(A_i + P + E_i) \quad (16)$$

$$\beta_j = 0.05 + 0.01(A_j + P + E_j) \quad (17)$$

where A is the descending present position command, P is the co-activation signal, and E is the stretch feedback from the spindles. The number of contractile fibers recruited into force are:

$$B_i = 0.2 + 2 \cdot (A_i + P + E_i) \quad (18)$$

$$B_j = 0.2 + 2 \cdot (A_j + P + E_j). \quad (19)$$

Renshaw population cell activity is modeled by

$$\frac{dR_i}{dt} = \phi(\lambda B_i - R_i)DA_5 z_i \max(M_i, 0) - DA_6 \cdot R_i(1.5 + \max(R_j, 0)) \quad (20)$$

$$\frac{dR_j}{dt} = \phi(\lambda B_j - R_j)DA_5 z_j \max(M_j, 0) - DA_6 \cdot R_j(1.5 + \max(R_i, 0)) \quad (21)$$

where the Renshaw cell recruitment rate z is:

$$z_i = 0.02(1 + \max(M_i, 0)) \quad (22)$$

$$z_j = 0.02(1 + \max(M_j, 0)) \quad (23)$$

and it depends on the level of α-MN activation. The α-MN population activity is described by the following equation

$$\frac{dM_i}{dt} = \phi(\lambda B_i - M_i) \cdot DA_7 \cdot (A_i + P + \chi \cdot E_i) - (M_i + 2) \cdot DA_8 \cdot (1 + \Omega \cdot \max(R_i, 0) + \rho \cdot \max(X_i, 0) + \max(I_j, 0)) \quad (24)$$

$$\frac{dM_j}{dt} = \phi(\lambda B_j - M_j) \cdot DA_7 \cdot (A_j + P + \chi \cdot E_j) - (M_j + 2) \cdot DA_8 \cdot (1 + \Omega \cdot \max(R_j, 0) + \rho \cdot \max(X_j, 0) + \max(I_i, 0)) \quad (25)$$

where X is the type I_b interneuron (I_bIN) force feedback and I is the type I_a interneuron. The type Ia interneuron (I_aIN) population activity is defined as

$$\frac{dI_i}{dt} = \phi \cdot (15 - I_i) \cdot DA_9 \cdot (A_i + P + \chi E_i) - DA_{10} \cdot I_i(1 + \Omega \cdot \max(R_i, 0) + \max(I_j, 0)) \quad (26)$$

$$\frac{dI_j}{dt} = \phi \cdot (15 - I_j) \cdot DA_9 \cdot (A_j + P + \chi E_j) - DA_{10} \cdot I_j(1 + \Omega \cdot \max(R_j, 0) + \max(I_i, 0)). \quad (27)$$

The I_bIN population activity is excited by feedback activity of force-sensitive Golgi tendon organs

$$\frac{dX_i}{dt} = \phi \cdot DA_{11}(15 - X_i)F_i - X_i \cdot DA_{11} \cdot (0.8 + 2.2\max(X_j, 0)) \quad (28)$$

$$\frac{dX_j}{dt} = \phi \cdot DA_{11}(15 - X_j)F_j - X_j \cdot DA_{11} \cdot (0.8 + 2.2\max(X_i, 0)). \quad (29)$$

The static γ-MN activity is described by

$$\frac{dS_i}{dt} = \phi(10 - S_i)(A_i + P) - S_i[1.8 + 0.2h(R_i)] \quad (30)$$

$$\frac{dS_j}{dt} = \phi(10 - S_j)(A_j + P) - S_j[1.8 + 0.2h(R_j)] \quad (31)$$

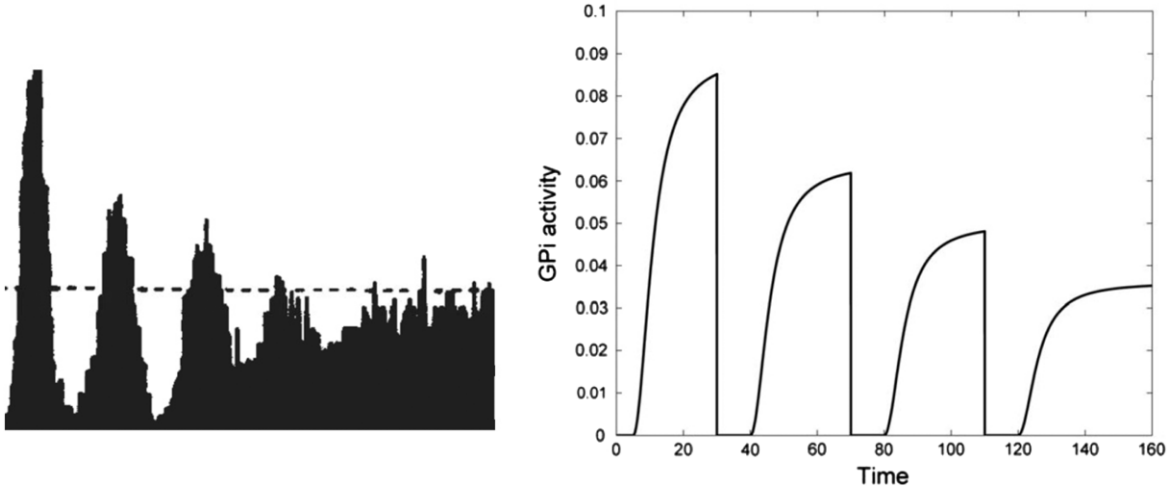

Fig. 2. Qualitative comparison of the experimental GPi post-stimulus time histogram (PSTH) in MPTP monkey (column 1; reproduced with permission from Tremblay et al., 1989, Fig. 2, p. 23, Copyright Elsevier) and simulated GPi activity used as input to the cortico-spinal model (column 2).

where $h(w) = \max(w, 0)/(0.3 + \max(w, 0))$. The intrafusal muscle contraction associated with static γ-MN activation is described by

$$\frac{dU_i}{dt} = 4S_i - U_i \tag{32}$$

$$\frac{dU_j}{dt} = 4S_j - U_j. \tag{33}$$

The dynamic γ-MN activity is

$$\frac{dD_i}{dt} = (8 - D_i)(100G[V_i]^+ + P) - (D_i + 1.2)(1 + 100G[V_j]^+ + 0.5h(R_i)) \tag{34}$$

$$\frac{dD_j}{dt} = (8 - D_j)(100G[V_j]^+ + P) - (D_j + 1.2)(1 + 100G[V_i]^+ + 0.5h(R_j)). \tag{35}$$

The intrafusal muscle contraction associated with dynamic γ-MN activation is

$$\frac{dN_i}{dt} = 4D_i - N_i \tag{36}$$

$$\frac{dN_j}{dt} = 4D_j - N_j. \tag{37}$$

The spindle receptor activation was defined as

$$\frac{dW_i}{dt} = (2 - W_i)(G_s \cdot [U_i + L_i - \Gamma_i]^+) + G_v \left(\left[N_i + \frac{dL_i}{dt} \right]^+ \right)^{0.3} - 10W_i \tag{38}$$

$$\frac{dW_j}{dt} = (2 - W_j)(G_s \cdot [U_j + L_j - \Gamma_i]^+) + G_v \left(\left[N_j + \frac{dL_j}{dt} \right]^+ \right)^{0.3} - 10W_j. \tag{39}$$

The stretch feedback signal is given by

$$E_i = a_e \cdot W_i \tag{40}$$

$$E_j = a_e \cdot W_j \tag{41}$$

where a_e is the feedback gain signal.

Table 1
Model parameters when an oscillatory GPi signal is used as input to the normally functioning cortico-spinal model. Dopamine levels in both cortex and spinal cord are normal.

Symbol	Value	Symbol	Value
g_0	0.09	T_2	0.3
k	1	Γ_i	21.01
η	0.4	Γ_F	1
I_m	1	ϕ	0.1
β	35.5	G_v	1
γ	1	G_s	1
δ	1	DA_1	1
χ	1	DA_2	1
Ω	1	DA_3	1
ρ	1	DA_4	1
α_e	1	DA_5	1
τ	5	DA_6	1
α_w	0.061	DA_7	1
B_u	0.02	DA_8	1
B_p	0.05	DA_9	1
λ	5	DA_{10}	1
T_1	0.75	DA_{11}	1

3. Results

3.1. Effects of an oscillatory globus pallidus internal segment signal as an input to a normally functioning cortico-spinal model of muscle activation

A qualitative comparison of the oscillatory cellular response of GPi neurons to striatal stimulation in MPTP-treated monkeys (Tremblay et al., 1989) and the simulated oscillatory GPi response is depicted in Fig. 2. In the Cutsuridis and Perantonis (2006) computational study such an oscillatory GPi signal was shown to generated a repetitive, but non-co-contractive pattern of antagonist muscle bursts (see Figure 10 in Cutsuridis & Perantonis, 2006) required to complete the movement.

In Figs. 3 and 4 such an oscillatory GO signal (GPi neuronal response) was used as an input to a normally functioning cortico-spinal model (i.e. dopamine was not depleted in cortex and spinal cord (DA values in Table 1 are set to 1)). A repetitive, but *non* co-contractive agonist–antagonist pattern is evident both at the cortical (DVV activity) and spinal (alpha motoneuronal activity) levels. The peak values and durations of each agonist–antagonist burst are progressively decreasing as the movement progresses (Doudet, Gross, Lebrun-Grandie, & Bioulac, 1985; Doudet et al., 1990; Hallett & Khoshbin, 1980; Vaillancourt et al., 2006, 2004).

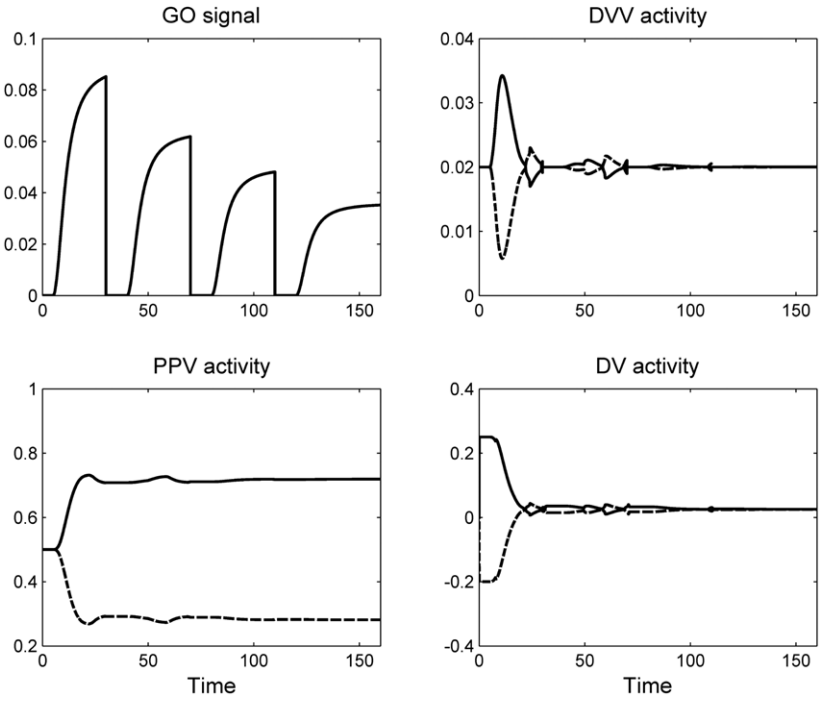

Fig. 3. Simulated abnormal GPi activity (row 1, column 1), DVV activity (row 1, column 2), PPV activity (row 2, column 1) and DV activity (row 2, column 2). Dopamine levels in cortex and spinal cord are normal (see Table 1 for parameter values). Multiple DVV peaks and PPV inflection points, representing additional motor commands necessary for completing the movement, can be observed. GO: globus pallidus internal segment activity; DVV: desired velocity vector; PPV: present position vector; DV: difference vector.

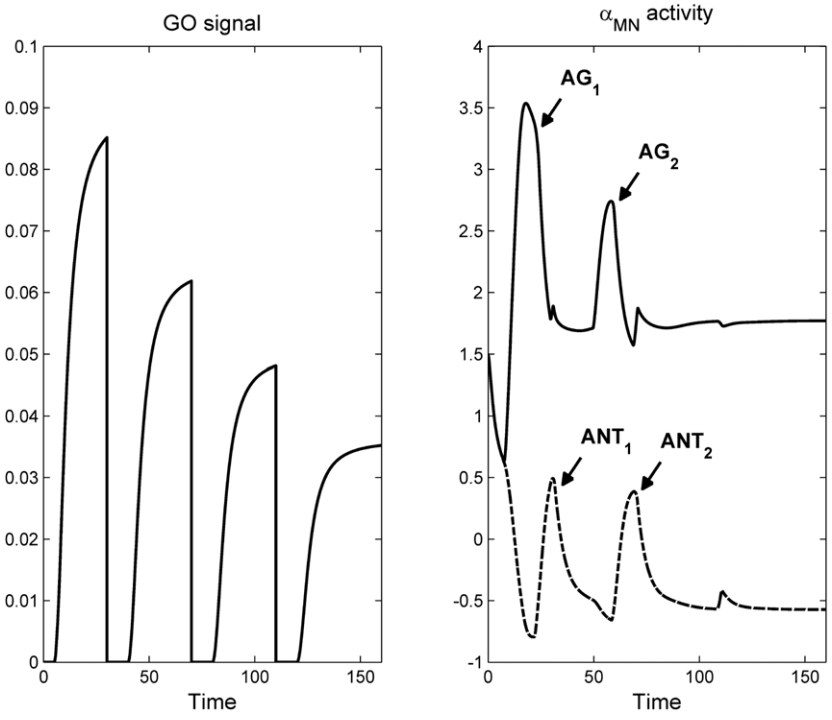

Fig. 4. Simulated abnormal GPi activity (column 1) and alpha motoneuronal activity (column 2) when dopamine levels in cortex and spinal cord are normal (see Table 1 for parameter values). A repetitive, *but not* co-contractive pattern of muscle activation (AG_1–ANT_1–AG_2–ANT_2) can be observed.

Fig. 5 shows the position, velocity and muscle force traces during the full movement amplitude. An overshoot of movement can be observed from the position (limb displacement) trace, which equilibrates at about 13 ms after movement onset (movement onset was calculated as the time where the displacement deviates from zero). The velocity profile is smooth and asymmetric. The deceleration time (i.e. the time from velocity peak value till the end of movement) is slightly longer than the acceleration time (i.e. time from movement onset till velocity peak value). From the muscle force trace, the agonist burst is followed few ms later by a smaller amplitude antagonist burst, which brings the limb to its final position.

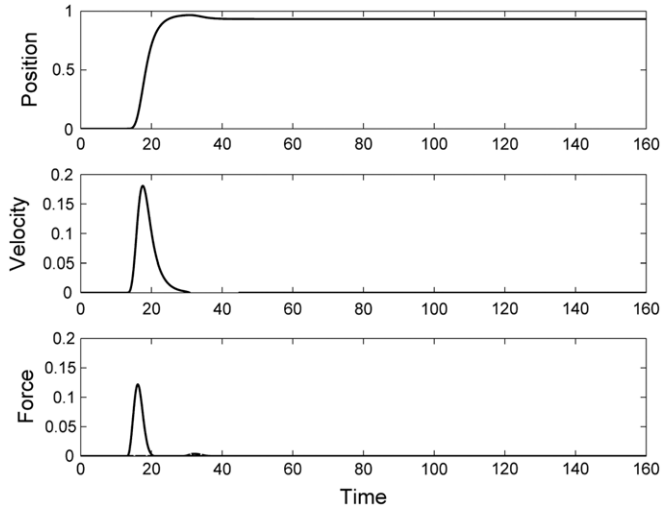

Fig. 5. Simulated forearm displacement (row 1), velocity profile (row 2) and muscle force (row 3) when an abnormal GPi activity (GO signal; see Fig. 2) signal is used as input to the cortico-spinal model (see Fig. 1). The dopamine levels in cortex and spinal cord are normal (see Table 1 for parameter values).

Table 2
Model parameters when an oscillatory GPi signal is used as input to the cortico-spinal model. Dopamine levels are depleted in cortex but held at normal levels in the spinal cord.

Symbol	Value	Symbol	Value
g_0	0.09	T_2	0.3
k	1	Γ_i	21.01
η	0.4	Γ_F	1
I_m	1	ϕ	0.1
β	35.5	G_v	1
γ	1	G_s	1
δ	1	DA_1	0.7
χ	1	DA_2	0.7
Ω	1	DA_3	0.7
ρ	1	DA_4	0.7
α_e	1	DA_5	1
τ	5	DA_6	1
α_w	0.061	DA_7	1
B_u	0.02	DA_8	1
B_p	0.05	DA_9	1
λ	5	DA_{10}	1
T_1	0.75	DA_{11}	1

3.2. Effects of an oscillatory GPi signal and dopamine depletion in cortex

The effects of the oscillatory GO signal (GPi neuronal response) and dopamine's depletion only in cortex are depicted in Fig. 6. A widespread dopaminergic innervation of the primate neocortex has been experimentally reported (Bjorklund & Lindvall, 1984; Williams & Goldman-Rakic, 1998) and recently reviewed by the Cutsuridis and Perantonis (2006) computational study. In the model, cortical dopamine depletion (see Fig. 6 and Table 2 for parameter values) results in an increase in background activity in primary motor cortex (DVV activity; Doudet et al., 1990; Watts & Mandir, 1992), a reduction in the peak values of both DVV agonist and antagonist activities (Doudet et al., 1990), and a decrease in their rate of change (Doudet et al., 1990). Also, a decrease in signal-to-noise ratio can be observed due to the loss of directional selectivity of cortical cells (Watts & Mandir, 1992). This loss causes cells that were not previously supposed to fire (e.g. in the non-dopamine depleted case), they do so now leading to much broader (in duration) agonist–antagonist pairs.

A similar loss of directional selectivity can be seen in the alpha motoneuronal level (see Fig. 7). Multiple bursts of EMG

Table 3
Model parameters when an oscillatory GPi signal is used as input to the cortico-spinal model. Dopamine levels are depleted in both cortex and spinal cord.

Symbol	Value	Symbol	Value
g_0	0.09	T_2	0.3
k	1	Γ_i	21.01
η	0.4	Γ_F	1
I_m	1	ϕ	0.1
β	35.5	G_v	1
γ	1	G_s	1
δ	1	DA_1	0.7
χ	1	DA_2	0.7
Ω	1	DA_3	0.7
ρ	1	DA_4	0.7
α_e	1	DA_5	0.7
τ	5	DA_6	0.7
α_w	0.061	DA_7	0.7
B_u	0.02	DA_8	0.7
B_p	0.05	DA_9	0.7
λ	5	DA_{10}	0.7
T_1	0.75	DA_{11}	0.7

ity (AG_1–ANT_1–AG_2–ANT_2–AG_3–ANT_3–AG_4–ANT_4) can be clearly seen (Benazzouz et al., 1992; Hallett & Khoshbin, 1980). An increase in the peak values of the agonist bursts (compare agonist peaks from Figs. 4 and 7) is evident due to the reduction of the antagonist burst peak values. The first agonist–antagonist pair is non-co-contractive, but every subsequent pair is co-contractive. Co-contraction of antagonist muscles (e.g. a bicep muscle and a tricep muscle during a flexion movement) adds an extra load (in addition to inertia and gravity) to the agonist muscle, which attempts to accelerate the limb and bring it as close as possible to the final position. Additional co-contractive pairs are then required to complete the movement (Hallett & Khoshbin, 1980).

As expected, Fig. 8 shows multiple inflection points (position trace) and peaks (velocity and muscle force traces) needed to bring the limb to its final position. Each position inflection point and velocity peal represents a distinct motor program. In this case four motor programs are required to complete the movement. Similarly from the muscle force trace, multiple muscle bursts can be seen. The first agonist burst overcomes inertia and accelerates the limb, while the remaining four progressively lower peaked co-contractive agonist–antagonist bursts bring the limb to its final position.

3.3. Effects of an oscillatory GPi activity and dopamine depletion in cortex and spinal cord in a model of movement generation

Dopamine depletion in the cortex and spinal cord results in no significant changes in neuronal activity (compare neuronal activities in Figs. 6 and 9). The presence of dopaminergic fibers in the spinal cord (both dorsal and ventral horns) has been observed by several groups (Bjorklund & Skagerberg, 1979; Blessing & Chalmers, 1979; Heise & Kayalioglu, 2008; Shirouzou, Anraku, Iwashita, & Yoshida, 1990; Weil-Fugazza & Godefroy, 1993). An excellent review of the dopaminergic innervations of the spinal cord can be found in Cutsuridis and Perantonis (2006).

Significant changes can be, however, observed in the alpha motoneuronal activity (see Fig. 10) and kinematic parameters (see Fig. 11). The peak value of both agonist and antagonist burst is reduced. Also, the rate of change of these bursts is increased. As before (see Fig. 7), the first agonist–antagonist burst is non-co-contractive, but every subsequent one is.

As in Fig. 8, multiple inflection points (position trace) and peaks (velocity and muscle force traces) are needed to complete the movement. In contrast to Fig. 8, the number of these peaks is reduced (from 4 to 2). Co-contraction of antagonist bursts can be seen only between the AG_2–ANT_1 pair.

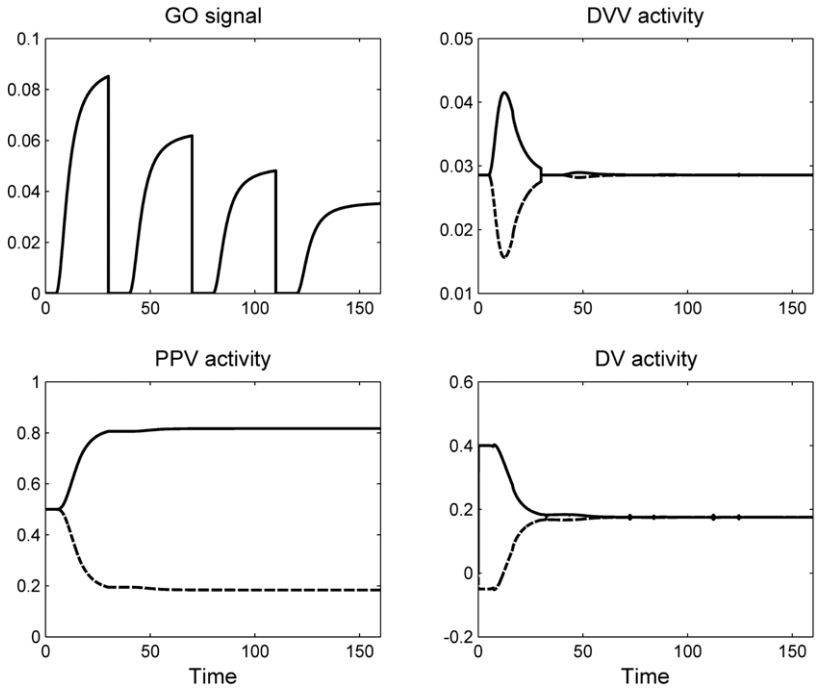

Fig. 6. Simulated abnormal GPi activity (row 1, column 1), DVV activity (row 1, column 2), PPV activity (row 2, column 1) and DV activity (row 2, column 2) when dopamine levels in cortex are depleted and dopamine levels in spinal cord are normal (see Table 2 for parameter values).

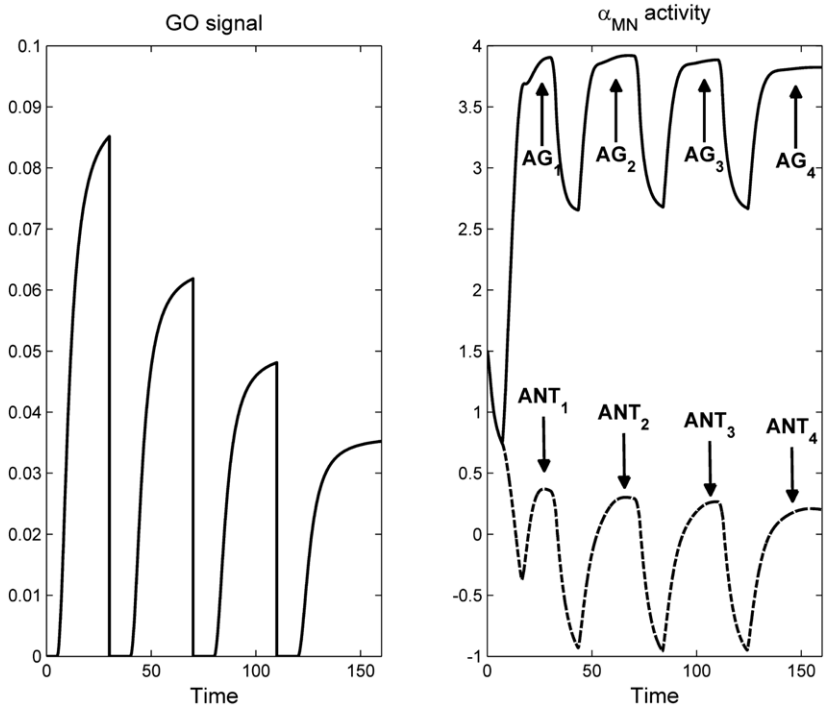

Fig. 7. Simulated abnormal GPi activity (column 1) and alpha motoneuronal activity (column 2) when dopamine levels in cortex are depleted and dopamine levels in spinal cord are normal (see Table 2 for parameter values). A repetitive *and* co-contractive pattern of muscle activation (AG_1–ANT_1–AG_2–ANT_2–AG_3–ANT_3–AG_4–ANT_4) can be observed.

4. Discussion

4.1. What have we learned from the model?

The present work is an extension of the Cutsuridis (2007) and Cutsuridis and Perantonis (2006) models of bradykinesia and rigidity to investigate the origins of the repetitive and co-contractive pattern of muscle activation in PD. Although these models were successful in simulating a wealth of neuronal, EMG and kinematic data from PD patients and MPTP-treated animals including a repetitive triphasic pattern of muscle activation, a reduction in the size and rate of development of the first agonist EMG burst, a prolongation of the behavioral reaction and movement time and movement variability, they failed to reproduce a repetitive *and* co-contractive pattern of antagonist muscles as it has been observed in PD patients (Pfann, Buchman,

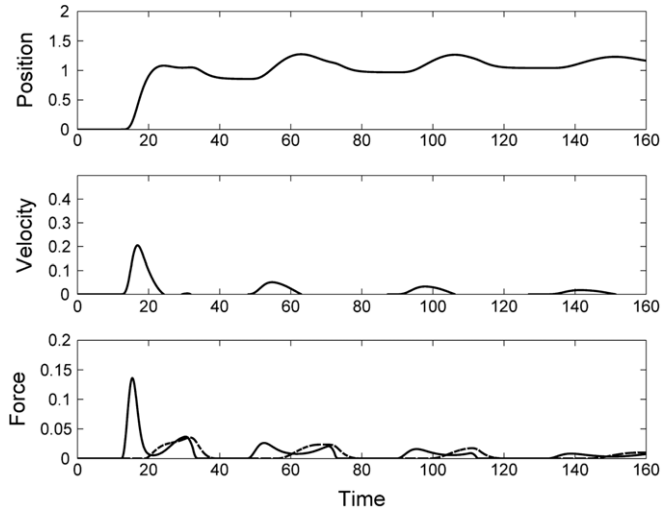

Fig. 8. Simulated forearm displacement (row 1), velocity profile (row 2) and muscle force (row 3) when an abnormal GPi activity (GO signal; see Fig. 2) signal is used as input to the cortico-spinal model (see Fig. 1) and dopamine levels in cortex are depleted. The dopamine levels in spinal cord are normal (see Table 2 for parameter values). Multiple peaks in the velocity and force profiles and multiple inflection points in the displacement curve are evident indicating the need for additional motor commands to bring the limb to the final position.

Comella, & Corcos, 2001; Vaillancourt et al., 2004, 2006) and MPTP-treated animals (Benazzouz et al., 1992; Doudet et al., 1990).

The present model is successful in simulating such a repetitive *and* co-contractive pattern if an oscillatory GPi signal drives a dopamine depleted cortical module and a normally functioning spinal one. If dopamine is also depleted in the spinal cord, then the size, duration and rate of development of the repetitive and co-contractive EMG bursts change, but the order of multiple agonist–antagonist bursts is preserved. On the other hand, if an oscillatory GPi signal drives a normally functioning cortico-spinal model, then a repetitive, but *non* co-contractive pattern of muscle activation arises. This means that dopamine depletion in the cortex and spinal cord is *solely* responsible for the co-contractive component of the muscle activation. This model prediction has important consequences in the development of PD therapies such as DA replacement in cortex and spinal cord, which can alleviate some impairments of PD such as slowness of movement (bradykinesia) and rigidity.

4.2. Model's assumptions and predictions are physiologically sound

The model has made several assumptions. First, it assumed an oscillatory GO signal representing the GPi activity, which comprised of at least two alternating excitation–inhibition regions and drove the model motor cortical cells. Similar abnormal oscillatory GPi responses have been observed experimentally by Tremblay et al. (1989) after injecting MPTP basal ganglia related structures in the monkey.

Second, the model assumed that both model cortical and spinal cord cells are innervated by dopamine. Such widespread innervations of the primate neocortex and spinal cord has been experimentally reported (Bjorklund & Lindvall, 1984; Bjorklund & Skagerberg, 1979; Blessing & Chalmers, 1979; Heise & Kayalioglu, 2008; Shirouzou et al., 1990; Weil-Fugazza & Godefroy, 1993; Williams & Goldman-Rakic, 1998) and recently reviewed by the Cutsuridis and Perantonis (2006) computational study. Briefly, the sources of the dopaminergic fibers in neocortex are the neurons of the substantia nigra (SN), the ventral tegmental area (VTA), and retrorubral area (RRA) (Williams & Goldman-Rakic, 1995). DA innervation is densest in the frontal areas (anterior cingulate (area 24) (Berger, Trottier, Verney, Gaspar, & Alvarez, 1988; Elsworth, Deutch, Redmond, Sladek, & Roth, 1990; Williams & Goldman-Rakic, 1998) and the motor areas (areas 4, 6, and SMA) (Berger et al., 1988; Elsworth et al., 1990; Gaspar, Duyckaerts, Alvarez, Javoy-Agid, & Berger, 1991; Gaspar, Stepniewska, & Kaas, 1992; Williams & Goldman-Rakic, 1998)). Intermediate density has been observed in the granular prefrontal (areas 46, 9, 10, 11, 12) (Gaspar et al., 1991, 1992; Scatton, Javoy-Agid, Rouquier, Dubois, & Agid, 1983), parietal (areas 1, 2, 3, 5, 7) (Lewis, Morrison, & Goldstein, 1988; Lidow, Goldman-Rakic, Gallager, Geschwind, & Rakic, 1989), temporal (areas 21, 22) (Berger et al., 1988), and

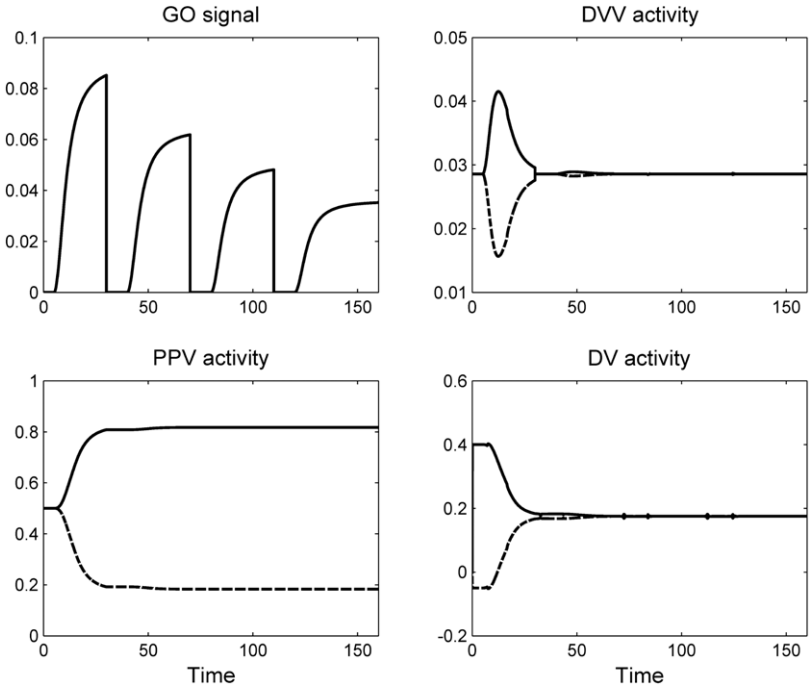

Fig. 9. Simulated abnormal GPi activity (row 1, column 1), DVV activity (row 1, column 2), PPV activity (row 2, column 1) and DV activity (row 2, column 2) when dopamine levels in cortex and spinal cord are depleted (see Table 3 for parameter values).

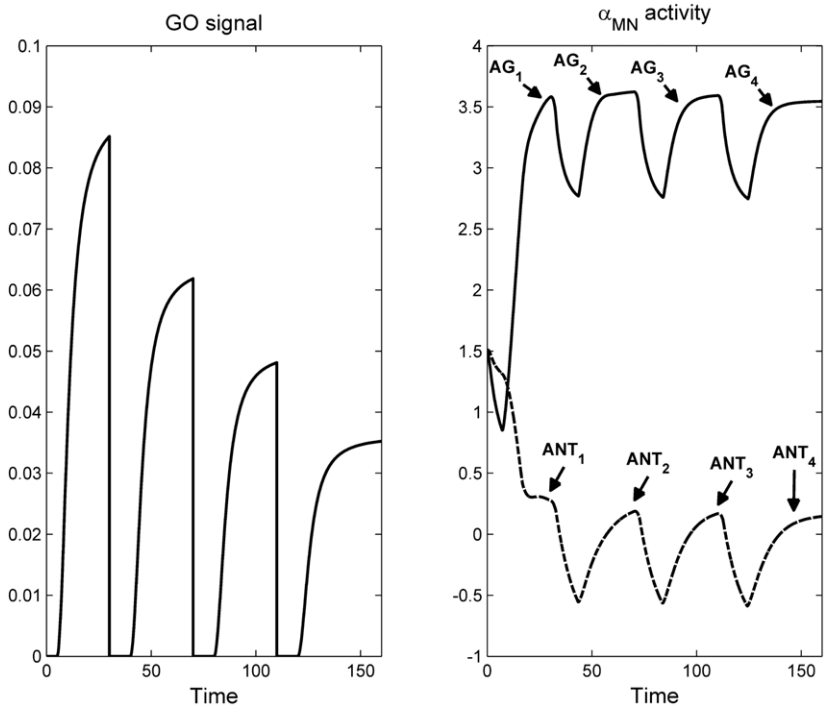

Fig. 10. Simulated abnormal GPi activity (column 1) and alpha motoneuronal activity (column 2) when dopamine levels in cortex and spinal cord are depleted (see Table 3 for parameter values). A repetitive *and* co-contractive pattern of muscle activation (AG_1–ANT_1–AG_2–ANT_2–AG_3–ANT_3–AG_4–ANT_4) can be observed. Due to dopamine depletion in spinal cord, the AG and ANT burst amplitudes and durations are decreased.

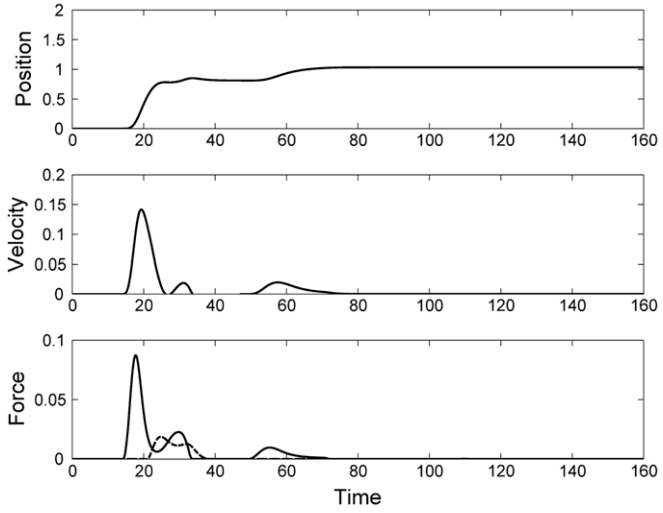

Fig. 11. Simulated forearm displacement (row 1), velocity profile (row 2) and muscle force (row 3) when an abnormal GPi activity (GO signal; see Fig. 2) signal is used as input to the cortico-spinal model (see Fig. 1) and dopamine levels in cortex and spinal cord are depleted (see Table 3 for parameter values). Multiple peaks in the velocity and force profiles and multiple inflection points in the displacement curve are evident indicating the need for additional motor commands to bring the limb to the final position.

posterior cingulate (area 23) (Berger et al., 1988) cortices. The lowest density is in primary visual cortex (area 17) (Berger et al., 1988). At the level of the spinal cord both dorsal and ventral horns have been shown to be innervated by dopamine (Bjorklund & Skagerberg, 1979; Blessing & Chalmers, 1979; Heise & Kayalioglu, 2008; Shirouzou et al., 1990; Weil-Fugazza & Godefroy, 1993; Commissiong, Gentleman, & Neff, 1979).

Finally, the model assumed that differential dopamine depletion of GPi and key motor cortical and spinal cord cells predicts the experimentally observed repetitive *and* co-contractive pattern of muscle activation in MPTP-treated monkeys (Benazzouz et al., 1992; Doudet et al., 1990) and PD patients (Hallett & Khoshbin, 1980; Pfann et al., 2001; Vaillancourt et al., 2004, 2006). The effects of dopamine depletion in basal ganglia, primary and supplementary motor cortex and spinal cord has been experimentally documented extensively (Benazzouz et al., 1992; Doudet et al., 1985, 1990; Tremblay et al., 1989; Watts & Mandir, 1992). Some of these findings include an oscillatory GPi neuronal response (Tremblay et al., 1989), a cellular disorganization in cortex (Doudet et al., 1990), an increase in neuronal baseline activity (Watts & Mandir, 1992), a reduction of firing intensity and firing rate of cells in primary motor cortex (Watts & Mandir, 1992) and a disinhibition of reciprocally tuned cells (Doudet et al., 1985, 1990).

4.3. Future work

A detailed basal ganglia (BG) model, which accounts for all the known detailed anatomical, neurochemical and neurophysiological evidence of basal ganglia structures, is currently being developed to study the conditions under which dopamine depletion in the basal ganglia structures give rise to the abnormal oscillatory GPi neuronal response observed after striatal stimulation in MPTP-treated animals (Tremblay et al., 1989). Several pathways (direct and indirect) and structures (globus pallidus external segment (GPe), subthalamic nucleus (STN), and substantia nigra pars compacta (SNc)) modulate the output striatal signal before it arrives in the GPi (Alexander, Crutcher, & DeLong, 1990). Furthermore, the hyperdirect pathway from the cortex to the STN is another source of modulation of the GPi neuronal response (Mink, 1996). Dopamine from the SNc innervates all of basal ganglia structures (striatum, GPe, STN, GPi, SNr) (Cantoze, Picconi, Gubellini, Bernadi, & Calabresi, 2001; Lavoie, Smith, & Parent, 1989) and the thalamic nuclei (García-Cabezas, Rico, Sánchez-González, & Cavada, 2007; García-Cabezas, Martínez-Sánchez, Sánchez-González, Garzón, & Cavada, 2009; Sánchez-González, García-Cabezas, Rico, & Cavada, 2005; Melchitzky, Erickson, & Lewis, 2006).

This BG model will later be added to a laminar model of the cortico-spinal circuitry to study the effects of dopamine depletion in key cortical and spinal neuronal types and their role in planning and execution of movement sequences in Parkinson's disease.

Acknowledgements

This work was supported by the NSF Science of Learning Center CELEST grant SMA-0835976, NIMH R01 MH61492, NIMH R01 MH60013 and NIMH Silvio Conte Center grant P50 MH71702.

References

Alexander, G. E., Crutcher, M. D., & DeLong, M. R. (1990). Basal ganglia-thalamocortical circuits: parallel substrates for motor, oculomotor, prefrontaland limbic functions. *Progress in Brain Research*, *85*, 119–146.

Benazzouz, A., Gross, C., Dupont, J., & Bioulac, B. (1992). MPTP induced hemiparkinsonism in monkeys: behavioral, mechanographic, electromyographic and immunohistochemical studies. *Experimental Brain Research*, *90*, 116–120.

Berger, B., Trottier, S., Verney, C., Gaspar, P., & Alvarez, C. (1988). Regional and laminar distribution of dopamine and serotonin innervation in the macaque cerebral cortex: a radioautographic study. *Journal of Comparative Neurology*, *273*, 99–119.

Bjorklund, A., & Lindvall, O. (1984). Dopamine containing systems in the CNS. In A. Bjorklund, & T. Hokfelt (Eds.), *Classical transmitters in the CNS, part 1*: *vol. 2. Handbook of chemical neuroanatomy* (pp. 55–121).

Bjorklund, A., & Skagerberg, G. (1979). Evidence of a major spinal cord projection from the diencephalic A11 dopamine cell group in the rat using transmitter-specific fluorescence retrograde tracing. *Brain Research*, *177*, 170–175.

Blessing, W. W., & Chalmers, J. P. (1979). Direct projection of catecholamine (presumably dopamine)-containing neurons from the hypothalamus to spinal cord. *Neuroscience Letters*, *11*, 35–40.

Britton, T., Thompson, P., Day, B., Rothwell, J., Findley, L., & Marsden, C. (1994). Rapid wrist movements in patients with essential tremor. The critical role of the second agonist burst. *Brain*, *117*, 39–47.

Brown, S. H., & Cooke, J. D. (1984). Initial agonist burst duration depends on movement amplitude. *Experimental Brain Research*, *55*, 523–527.

Brown, S. H., & Cooke, J. D. (1990a). Movement related phasic muscle activation I. Relations with temporal profile of movement. *Journal of Neurophysiology*, *63*(3), 455–464.

Brown, S. H., & Cooke, J. D. (1990b). Movement related phasic muscle activation II. Generation and functional role of the triphasic pattern. *Journal of Neurophysiology*, *63*(3), 465–472.

Camarata, P. J., Parker, R. G., Park, S. K., Haines, S. J., Turner, D. A., Chae, H., et al. (1992). Effects of MPTP induced hemiparkinsonism on the kinematics of a two-dimensional, multi-joint arm movement in the rhesus monkey. *Neuroscience*, *48*(3), 607–619.

Berardelli, A., Dick, J. P. R., Rothwell, J. C., Day, B. L., & Marsden, C. D. (1986). Scaling of the size of the first agonist EMG burst during rapid wrist movements in patients with Parkinson's disease. *Journal of Neurology Neurosurgery & Psychiatry*, *49*, 1273–1279.

Cantoze, D., Picconi, B., Gubellini, P., Bernadi, G., & Calabresi, P. (2001). Dopaminergic control of synaptic plasticity in dorsal striatum. *European Journal of Neuroscience*, *13*(6), 1071–1077.

Commissiong, J. W., Gentleman, S., & Neff, N. H. (1979). Spinal cord dopaminergic neurons: evidence for an uncrossed nigrostriatal pathway. *Neuropharmacology*, *18*, 565–568.

Cutsuridis, V. (2007). Does reduced spinal reciprocal inhibition lead to co-contraction of antagonist motor units? A modeling study. *International Journal of Neural Systems*, *17*(4), 319–327.

Cutsuridis, V. (2006). Neural model of dopaminergic control of arm movements in Parkinson's disease bradykinesia. In S. Kolias, A. Stafilopatis, & W. Duch (Eds.), *LNCS*: *vol. 4131. ICANN 2006: artificial neural networks* (pp. 583–591). Berlin: Springer-Verlag.

Cutsuridis, V. (2010). Neural network modeling of voluntary single joint movement organization. II. Parkinson's disease. In W. A. Chaovalitwongse, P. Pardalos, & P. Xanthopoulos (Eds.), *Computational neuroscience* (pp. 193–212). Springer-Verlag.

Cutsuridis, V., & Perantonis, S. (2006). A neural model of Parkinson's disease bradykinesia. *Neural Networks*, *19*(4), 354–374.

Doudet, D. J., Gross, C., Arluison, M., & Bioulac, B. (1990). Modifications of precentral cortex discharge and EMG activity in monkeys with MPTP induced lesions of DA nigral lesions. *Experimental Brain Research*, *80*, 177–188.

Doudet, D. J., Gross, C., Lebrun-Grandie, P., & Bioulac, B. (1985). MPTP primate model of Parkinson's disease: a mechanographic and electromyographic study. *Brain Research*, *335*, 194–199.

Elsworth, J. D., Deutch, A. Y., Redmond, D. E., Sladek, J. R., & Roth, R. H. (1990). MPTP reduces dopamine and norepinephrine concentrations in the supplementary motor area and cingulate cortex of the primate. *Neuroscience Letters*, *114*, 316–322.

García-Cabezas, M. A., Martínez-Sánchez, P., Sánchez-González, M. A., Garzón, M., & Cavada, C. (2009). Dopamine innervations in the thalamus: monkey versus rat. *Cerebral Cortex*, *19*(2), 424–434.

García-Cabezas, M. A., Rico, B., Sánchez-González, M. A., & Cavada, C. (2007). Distribution of the dopamine innervations in the macaque and human thalamus. *NeuroImage*, *34*(3), 965–984.

Gaspar, P., Duyckaerts, C., Alvarez, C., Javoy-Agid, F., & Berger, B. (1991). Alterations of dopaminergic and noradrenergic innervations in motor cortex in Parkinson's disease. *Annals of Neurology*, *30*, 365–374.

Gaspar, P., Stepniewska, I., & Kaas, J. H. (1992). Topography and collateralization of the dopaminergic projections to motor and lateral prefrontal cortex in owl monkeys. *Journal of Comparative Neurology*, *325*, 1–21.

Ghez, C., & Gordon, J. (1987a). Trajectory control in targeted force impulses. I. Role in opposing muscles. *Experimental Brain Research*, *67*, 225–240.

Ghez, C., & Gordon, J. (1987b). Trajectory control in targeted force impulses. II. Pulse height control. *Experimental Brain Research*, *67*, 241–252.

Ghez, C., & Gordon, J. (1987c). Trajectory control in targeted force impulses. III. Compensatory adjustments for initial errors. *Experimental Brain Research*, *67*, 253–269.

Godaux, E., Koulischer, D., & Jacquy, J. (1992). Parkinsonian bradykinesia is due to depression in the rate of rise of muscle activity. *Annals of Neurology*, *31*(1), 93–100.

Gottlieb, G. L., Latash, M. L., Corcos, D. M., Liubinskas, A. J., & Agarwal, G. C. (1992). Organizing principle for single joint movements: I. Agonist–antagonist interactions. *Journal of Neurophysiology*, *13*(6), 1417–1427.

Hallett, M., & Khoshbin, S. (1980). A physiological mechanism of bradykinesia. *Brain*, *103*, 301–314.

Hallett, M., & Marsden, C. D. (1979). Ballistic flexion movements of the human thumb. *Journal of Physiology*, *294*, 33–50.

Hallett, M., Shahani, B. T., & Young, R. R. (1975). EMG analysis of stereotyped voluntary movements in man. *Journal of Neurology Neurosurgery & Psychiatry*, *38*, 1154–1162.

Heise, C., & Kayalioglu, G. (2008). Cytoarchitecture of the spinal cord. In C. Watson, G. Paxinos, & G. Kayaliyoglu (Eds.), *The spinal cord*. London: Elsevier.

Lavoie, B., Smith, Y., & Parent, A. (1989). Dopaminergic innervation of the basal ganglia in the squirrel monkey as revealed by tyrosine hydroxylase immunohistochemistry. *Journal of Comparative Neurology*, *289*(1), 36–52.

Lewis, D. A., Morrison, J. H., & Goldstein, M. (1988). Brainstem dopaminergic neurons project to monkey parietal cortex. *Neuroscience Letters*, *86*, 11–16.

Lidow, M. S., Goldman-Rakic, P. S., Gallager, D. W., Geschwind, D. H., & Rakic, P. (1989). Distribution of major neurotransmitter receptors in the motor and somatosensory cortex of the rhesus monkey. *Neuroscience*, *32*(3), 609–627.

Melchitzky, D. S., Erickson, S. L., & Lewis, D. A. (2006). Dopamine innervation of the monkey mediodorsal thalamus: location of projection neurons and ultrastructural characteristics of axon terminals. *NeuroImage*, *143*(4), 1021–1030.

Mink, J. W. (1996). The basal ganglia: focused selection and inhibition of competing motor programs. *Progress in Neurobiology*, *50*, 381–425.

Pfann, K. D., Buchman, A. S., Comella, C. L., & Corcos, D. M. (2001). Control of movement in Parkinson's disease. *Movement Disorders*, *16*(6), 1048–1065.

Pfann, K. D., Hoffman, D. S., Gottlieb, G. L., Strick, P. L., & Corcos, D. M. (1998). Common principles underlying the control of rapid, single degree-of-freedom movements at different joints. *Experimental Brain Research*, *118*(1), 35–51.

Sánchez-González, M. A., García-Cabezas, M. A., Rico, B., & Cavada, C. (2005). The primate thalamus is a key target for brain dopamine. *Journal of Neuroscience*, *25*(26), 6076–6083.

Scatton, B., Javoy-Agid, F., Rouquier, L., Dubois, B., & Agid, Y. (1983). Reduction of cortical dopamine, noradrenaline, serotonin and their metabolites in Parkinson's disease. *Brain Research*, *275*, 321–328.

Shirouzou, M., Anraku, T., Iwashita, Y., & Yoshida, M. (1990). A new dopaminergic terminal plexus in the ventral horn of the rat spinal cord. Immunohistochemical studies at the light and the electron microscopic levels. *Experientia*, *46*, 201–204.

Stein, R. (1982). What muscle variable(s) does the nervous system control in limb movements? *Behavioral and Brain Sciences*, *5*, 535–577.

Tremblay, L., Filion, M., & Bedard, P. J. (1989). Responses of pallidal neurons to striatal stimulation in monkeys with MPTP-induced parkinsonism. *Brain Research*, *498*(1), 17–33.

Vaillancourt, D. E., Prodoehl, J., Sturman, M. M., Bakay, R. A., Veragen-Metman, L., & Corcos, D. M. (2006). Effects of deep brain stimulation and medication on strength, bradykinesia and electromyographic patterns of the ankle joint in Parkinson's disease. *Movement Disorders*, *21*(1), 50–58.

Vaillancourt, D. E., Prodoehl, J., Veragen-Metman, L., Bakay, R. A., & Corcos, D. M. (2004). Effects of deep brain stimulation and medication on bradykinesia and muscle activation in Parkinson's disease. *Brain*, *127*, 491–504.

Watts, R. L., & Mandir, A. S. (1992). The role of motor cortex in the pathophysiology of voluntary movement deficits associated with Parkinsonism. *Neurologic Clinics*, *10*(2), 451–469.

Weil-Fugazza, J., & Godefroy, F. (1993). Dorsal and ventral dopaminergic innervation of the spinal cord: functional implications. *Brain Research Bulletin*, *30*, 319–324.

Wierzbicka, M. M., Wiegner, A. W., & Shahani, B. T. (1986). Role of agonist and antagonist muscles in fast arm movements in man. *Experimental Brain Research*, *63*, 331–340.

Williams, S. M., & Goldman-Rakic, P. S. (1998). Widespread origin of the primate mesofrontal dopamine system. *Cerebral Cortex*, *8*, 321–345.

Williams, S. M., & Goldman-Rakic, P. S. (1995). Characterization of the dopaminergic innervation of the primate frontal cortex using a dopamine-specific antibody. *Cerebral Cortex*, *3*, 199–222.